The Damper Cage in Synchronous Generators with Hybrid Permanent Magnet for Hydropower Applications

The Damper Cage in Synchronous Generators with Hybrid Permanent Magnet for Hydropower Applications

Emir Poskovic
Energy Department
Politecnico di Torino
Torino, Italia
emir.poskovic@polito.it

Alex Lucco Borlera
R&D Department
SicmeOrange1 s.r.l.
Torino, Italia
alucco@orange1.eu

Luca Ferraris
Energy Department
Politecnico di Torino
Torino, Italia
luca.ferraris@polito.it

Silvio Vaschetto
Energy Department
Politecnico di Torino
Torino, Italia
silvio.vaschetto@polito.it

Alberto Tenconi
Energy Department
Politecnico di Torino
Torino, Italia
alberto.tenconi@polito.it

***Abstract*— Using hybrid coils, regulating Permanent magnet Synchronous Generators without electronic conversion devices is possible. These coils are placed around the magnets and regulate the voltage and power factors. On the other hand, the presence of damper winding required a preliminary study concerning the combination and operation of two winding systems on the rotor. Several configurations are analyzed using the finite element method, and different parameters are considered to select the most promising one.**

Keywords*— *Hybrid Permanent Magnet, Damper Winding, Synchronous Generator, Hydropower, Hybridization

I. INTRODUCTION

The hybridization of permanent magnets in electrical machines has recently aroused interest, especially for performance regulation in the flux-weakening range [1-4]. Commonly, serial and parallel arrangements have been applied in variable flux memory machines where the strong (NdFeB) and the weaker (AlNiCo or HMC [5],[6]) permanent magnets have been used [7]. Another way to realize these arrangements is by using particular coils [8]. The placement in the magnetic core of the coils depends on the regulation's aim and the machine's type.

In the case of the permanent magnet synchronous generator (PMSG) [9-12], connected directly online without a gearbox and electronic power conversion devices, the hybridization coils show a new solution for voltage regulation. The regulation in SG consists of an interval of RMS voltage variation of about 10%, considering power factor and reactive power condition. The hybridization coils are placed on the rotor close to permanent magnets to maximise voltage regulation. Another important aspect of the use of hybridization is the cost savings, considering the missing gearbox and inverter, even if the permanent magnets in NdFeb are expensive.

On the other hand, the use of hybridization meets a critical point: other coils are placed on the rotor as damper winding or cage. This winding is constituted of low-resistance bars and shorting circuit rings. The function of damper winding consists of different uses: suppressing hunting oscillations due to the variation of the load or frequency of the machine, maintaining balanced voltages under unbalanced loading, providing braking torque for the generator during the fault, starting operation for synchronous motors and condenser, reducing the parasitic harmonic [13-16]. In that context, maintaining the total harmonic distortion (THD) under the required value (5%) is one of the aims [17],[18]. Also, the damper cage current is affected by the open slot geometry of the stator, which leads to specific variations of magnetic flux in the air gap [19]. Considering all aspects mentioned above, the appropriate design and control strategy between hybridization and damper cage must be studied in detail.

The implementation of the control strategy consists of the position of both types of coils. The location of hybridization coils is almost identical to wound rotor synchronous machines (WRSM) [20], using the brushes and slip-rings arrangements to provide the DC supply. This solution produces sparking and maintenance problems. In this context, using brushless exciter [21-24] can resolve the mentioned drawbacks. However, brushless excitation can increase the cost and size of the generator and also can have the presence of electronic power conversion devices. In that way, the proposed solution is not connected directly online. Instead, an automatic voltage regulator (AVR) and rectifier connect the hybridisation coils through brushes and slip rings and permit their control. In general, the alternating current (AC) AVR has a control circuit, as in many cases, it is a microcontroller; it is not to be confused with an inverter system for power conversion.

In the proposed work, the effects of the damper cage have been studied for a hybrid permanent magnet synchronous generator (HPMSG) used in small hydropower applications. The generator is connected directly online with the use of an AVR, and the inverter is not used, as shown in Fig. 1. The assessment of different damper winding configurations has been proposed. The activity was developed with SicmeOrange1 company, which has much experience producing hydroelectric generators.

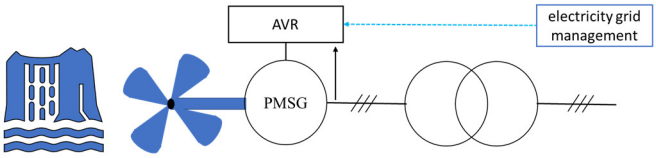

Fig. 1. Hybrid permanent magnet synchronous generator (PMSG): connected directly online and controlled by an automatic voltage regulator

II. Hybrid Permanent Magnet Synchronous Generator

The generator with hybrid coils and V-type permanent magnets is selected for this study. The machine operates totally submerged with a Kaplan turbine for a rated power of 278 kW with the hybridization coils not activated (the current density for hybridization coils is J=0 A/mm^2). At the same condition, the rated torque is 11028 Nm. The permanent magnets are sintered NdFeB with a remanence of 1.13 T, and hybridization coils are embedded in series arrangements near the magnets. The maximum current density for hybridization coils J is 4 A/mm^2, while for the stator windings is 4.5 A/mm^2. In the case of the positive arrangement (J=4 A/mm^2), the power reaches the value of 286 kW and torque 11358 Nm. Also, the voltage regulation of the RMS values is 24.7 V, more than ±5% of the rated voltage.

In the case of a submerged electrical machine, the proposed current density values guarantee safe thermal operation in ordinary conditions. The design and characteristics of HPMSG are reported in Fig. 2 and Table I. The hybridization coils are defined, but the damper cages, position, number and operation are studied hereafter. Therefore, modified rotor geometries will be proposed based on the described design. The following analysis is carried out by the finite element method [25],[26] in the Flux Altair environment, and the operation condition consists of maintaining the synchronism after a perturbation.

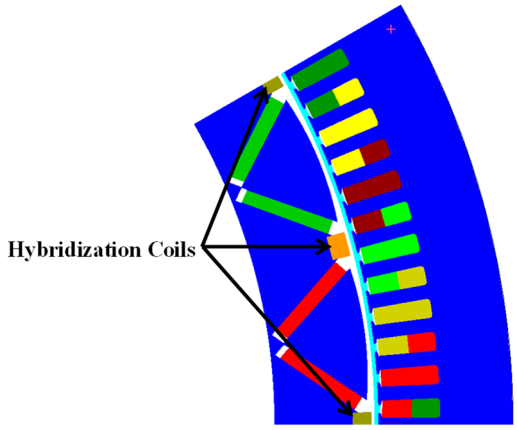

Fig. 2. HPMSG geometry design

Table I. Design Data of the HPMSG

Number of Poles	24
Number of Slots	144
Rated Current	410 A
Rated Power	278 kW
Rated Speed	250 RPM
Rated Torque	11028 Nm
Current Density	4.5 A/mm^2
Max operating temperature	80÷90°C
Air Gap	4 mm

III. Damper Cage in Hybrid Permanent Magnet Synchronous Generator

Several configurations and combinations of damper cages with hybrid coils are proposed. The exam was conducted taking into account the damper cage current (magnitude and exhaustion), harmonic content and THD for line-to-line no-load voltage, damper cage joule losses and Lorentz force related to the damper cage.

A. *First case: hybridization coils are connected in a shorting circuit*

In the proposed case, the hybridization coils are connected in a shorting circuit during the load or frequency variation or in the presence of a fault. In this context, the hybrid coils operate like a damper cage, as shown in Fig. 3. The line-to-line voltage and relative harmonic content are shown in Fig. 4. The first harmonic is 511.08 V, and THD is 0.78%. The transitory trend of the total damper winding current at the rated condition is shown in Fig. 5. The perturbation causes high current values, and the current is not completely reduced after 0.12 s. The joule losses in the damper cage depend on magnetic flux variation in the air gap due to the slot opening. The variation is generally high if the ratio between slot width and airgap thickness is high and the effect on the induced current in the damper cage is significant. They are not exhausted after perturbation and remain present at steady-state conditions. The damper cage losses are 2.76 W and 29.40 W at no-load and rated load conditions, respectively. The maximum Lorentz force the damper cage produces to provide braking torque is 844 N. The force is considered at the no-load operation to evaluate only the effect of the damper cage.

In the end, the proposed solution shows positive aspects concerning the THD and damper cage losses; however, the very high current values, 9208 A, do not allow this configuration to be used due to heating problems [27]. Other configurations will be analysed, considering the drawbacks mentioned above.

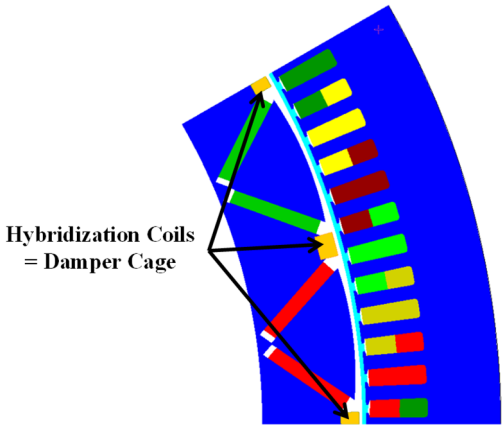

Fig. 3. HPMSG with hybrid coils used as damper cage

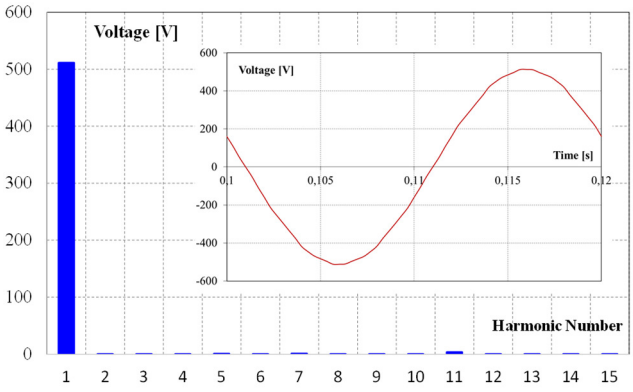

Fig. 4. No-load linked voltage and relative harmonic content for HPMSG where hybrid coils are damper cage

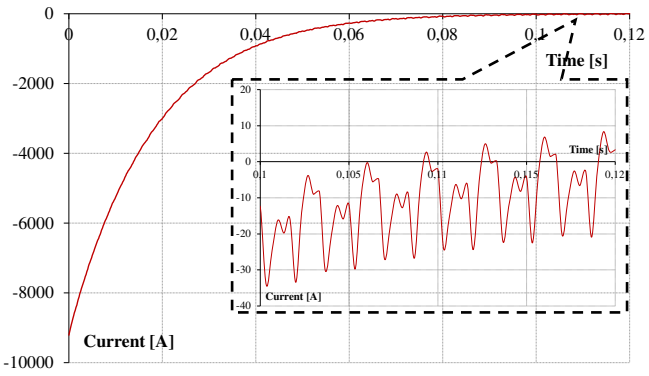

Fig. 5. Total current of the damper cage in the case of hybrid coils used as damper cage

B. *Second case: 7 damper cage bars for the magnet pole and no hybridization coils*

The 7 damper cage bars are implanted in the pole piece between the two magnets that form the V-type. The hybrid coils are not applied in this configuration (open circuit). The design is illustrated in Fig. 6. The total damper cage current shows very low values with respect to the previous case, as reported in Fig. 8. The transitory of such current is reduced after 0.064 s; however, the current oscillations due to slot opening produce permanent losses of about 68.64 W at no-load and 124.32 W for rated condition. The section of bars is lower compared to the previous case, and the bars' position on the rotor pole arc affects the losses and THD values. Therefore, the THD in the proposed case is 1.96%, and the first harmonic is 509.40 V, as reported in Fig. 7. Both values are worse with respect to the previous case due to adding the bars.

On the other hand, the maximum force for braking torque is 1552.5 N. The significant change in value with respect to the previous case is due to the higher magnetic induction that afflicts the damper cage compared to the hybrid coils. The damper windings are embedded in the rotor surface, while the hybrid coils are positioned close to the air gap.

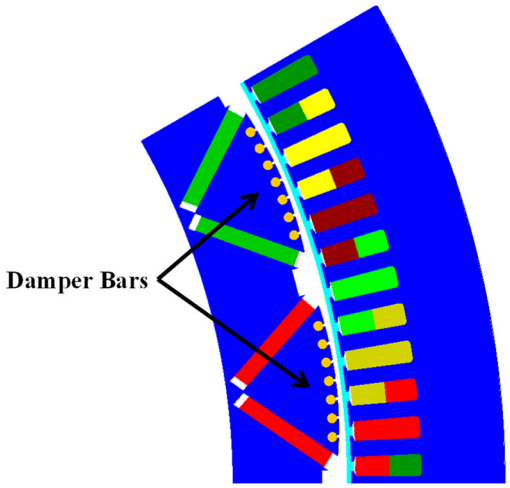

Fig. 6. PMSG with 7 damper bars for a magnet pole without the hybrid coils

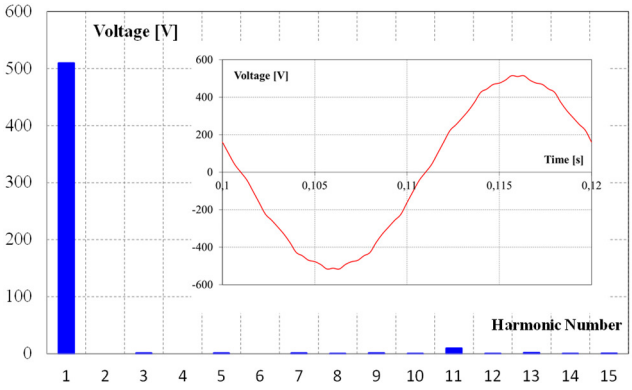

Fig. 7. No-load linked voltage and relative harmonic content for PMSG without hybrid coils

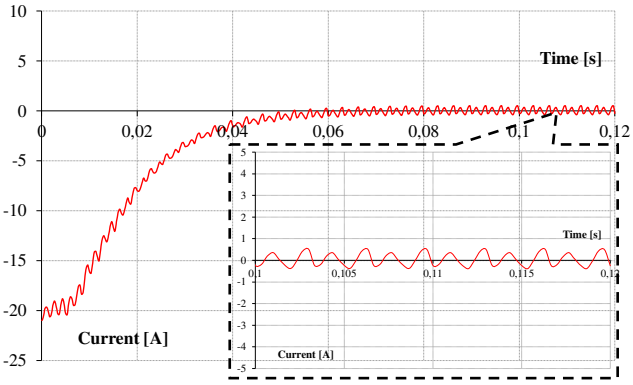

Fig. 8. Total current of the damper cage in the case of 7 damper bars for a magnet pole (no hybrid coils)

C. *Third case: 7 damper bars and hybridization coils in a shorting circuit*

The hybrid coils and 7 bars are connected together in a shorting circuit during the perturbation, as shown in Fig. 9. The THD value of 2.13% is increased compared to the second case. The first harmonic is reduced, 502.84 V, as shown in Fig. 10. The further variation of the magnetic path slightly worsens the THD value; however, the value remains significantly lower compared to the threshold of 5%. The total current of the damper configuration shows very high values (Fig. 11), which makes the heating phenomenon unsustainable for the designed machine. Moreover, the current transitory trend has not been completed. The damper cage joule losses are 147.96 W for no-load and 214.44 W for full load, respectively. The maximum force is 1662.3 N.

The only positive aspect is the increment of the braking effect; however, the high damper cage current value, 5514 A, produces serious thermal problems. For this reason, in the following cases, the hybrid coils will be maintained open to avoid the high current until the time 0.1 s; after that, the same hybridization circuit coils will be closed.

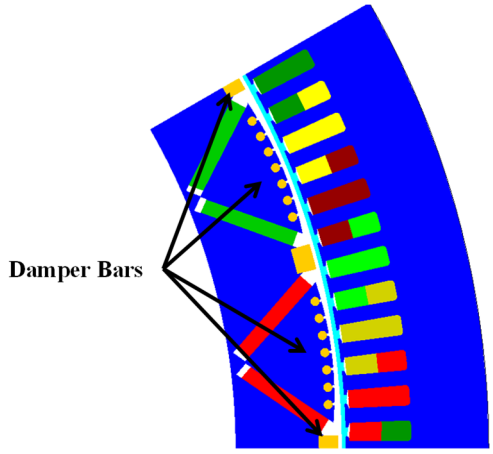

Fig. 9. HPMSG with 7 damper bars and hybridization coils in a shorting circuit

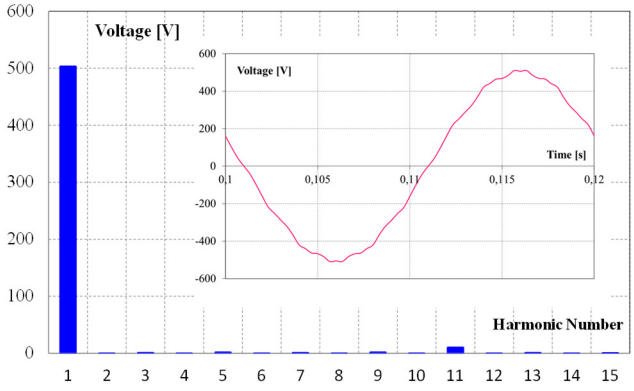

Fig. 10. No-load linked voltage and relative harmonic content for HPMSG with 7 damper bars and hybridization coils in a shorting circuit

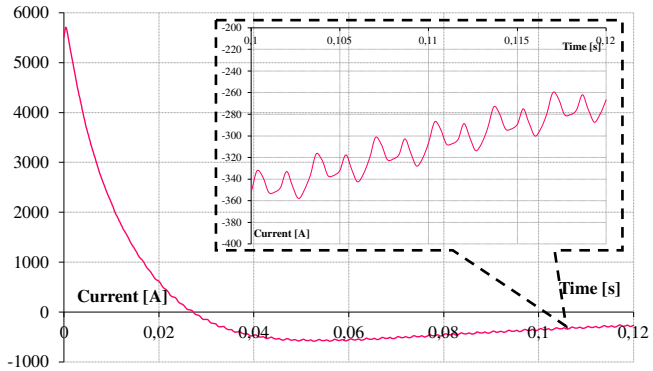

Fig. 11. Total current of the damper cage in the case of 7 damper bars and hybridization coils in a shorting circuit

D. Fourth case: 7 damper bars with delayed activation of hybridization

The damper cage is composed of only 7 bars, and hybridization coils are closed after 0.1 s from perturbation. It is possible due to the strategy control implemented using an AVR. The HPMSG with 7 damper winding for a magnet pole is shown in Fig. 12. The proposed configuration is affected by hybridization, which allows the voltage to be regulated. For this reason, the effect of the maximum positive and maximum negative arrangements will be investigated.

The harmonic content is shown in Fig. 13 and permits the determination of the THD values: positive arrangement PA→ 2.10%, J=0→ 1.95%, and negative arrangement NA → 2.01%. The THD value is better for zero hybridisation current, but the hybrid regulation maintains the THD in a more than acceptable interval between 1.90÷2.10%. On the other hand, the first harmonic variation due to hybridization is described hereafter: PA→ 528.32 V, J=0→ 509.40 V, negative arrangement NA→ 489.53 V. The positive regulation increases the voltage and permits a maximum delta variation of the RMS ΔV of 38.78 V.

The transient of the current is over at 0.058 s, as reported in Fig. 14. The maximum damper current is 20.7 A. The effect of hybridization affects the steady-state joule losses of the damper cage at no-load operation: PA→ 72.84 W, J=0→ 68.64 W, NA→ 63.96 W. The same happened for rated load operation: PA→ 125.64 W, J=0→ 124.32 W, NA→ 123.00 W. The maximum force for braking is 1552.6 N.

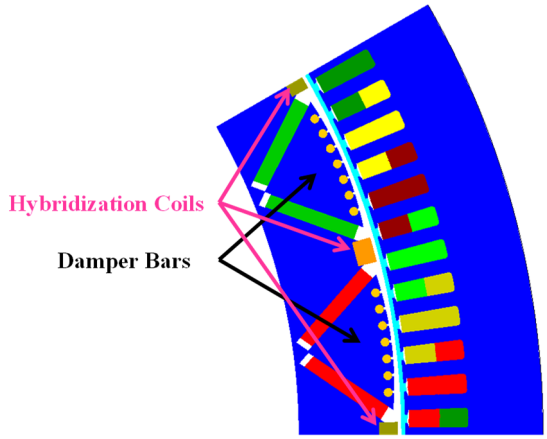

Fig. 12. HPMSG with 7 damper bars with delayed activation of hybridization

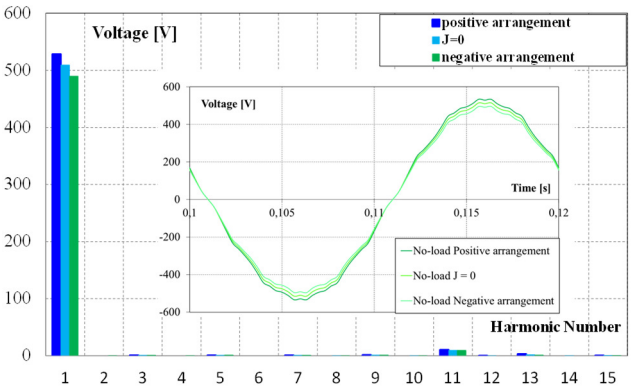

Fig. 13. No-load linked voltage and relative harmonic content for HPMSG with 7 damper bars with delayed activation of hybridization

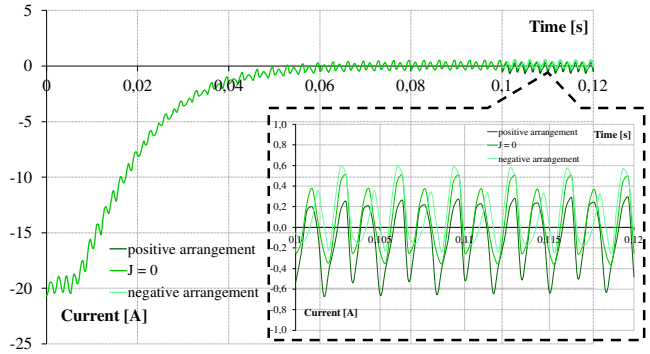

Fig. 14. Total current of the damper cage in the case of 7 damper bars with delayed activation of hybridization

E. *Fifth case: 5 damper bars with delayed activation of hybridization*

It is similar to the previous case; the only difference consists of the 5 damper windings for a magnet pole. The damper cage bar has the same section as the previous case. The reduction of bars will always keep a total negative number. The generator's design is shown in Fig. 15. The decrease in bar numbers allows the reduction of the joule losses but also affects the THD and maximum force.

From Fig. 16, the THD values are determined: PA→ 1.67%, J=0→ 1.54%, and NA→ 1.59%. Again, the lower THD value is for no current in hybrid coils, but all values are minor compared to the fourth case. Also, the first harmonics are higher: PA→ 529.39 V, J=0→ 510.42 V, and NA→ 490.50 V. In practice, an increment of 1 Volt has been noted with reducing the bar numbers. The maximum delta variation of the RMS ΔV is 38.89 V; compared to the value in the fourth case, the increase is almost negligible.

The damper current, reported in Fig. 17, shows a slight increment, and the maximum value is 30.7 A. The current transitory is over at 0.04 s. The lower number of damper bars reduces the damper cage losses, and for no-load operation are PA→ 48.72 W, J=0→ 45.12 W, and NA→ 41.76 W; while for rated load are PA→ 85.80 W, J=0→ 84.24 W, and NA→ 83.16 W. The maximum force for braking during perturbations is 1927.6 N. The increase in value corresponds to the increment of the damper cage current.

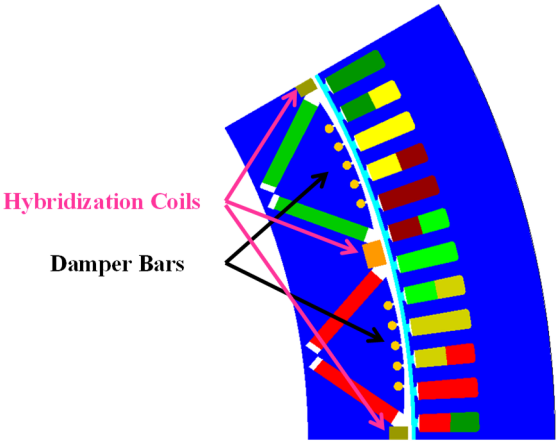

Fig. 15. HPMSG with 7 damper bars with delayed activation of hybridization

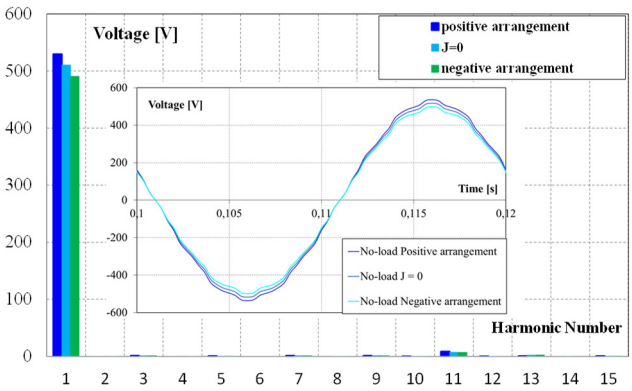

Fig. 16. No-load linked voltage and relative harmonic content for HPMSG with 5 damper bars with delayed activation of hybridization

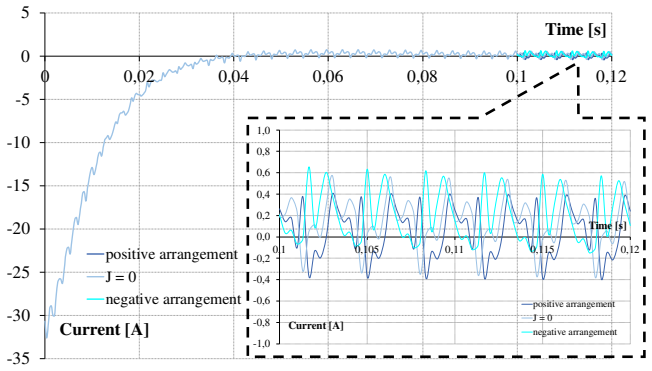

Fig. 17. Total current of the damper cage in the case of 5 damper bars with delayed activation of hybridization

F. *Sixth case: 9 damper bars with delayed activation of hybridization*

The 9 damper winding for a magnet pole is applied; other rotor geometry remains the same, as shown in Fig. 18. In Fig. 19, the first harmonics at no-load conditions are reported: PA→ 519.08 V, J=0→ 501.42 V, and NA→ 483.02 V. All values are decreased compared to fourth and fifth solutions of about ten volts. The reason is that the magnetic material located at the rotor edges is reduced to increase the number of bars. On the other hand, the THD values remain higher compared to the case with 7 damper bars: PA→ 1.87%, J=0→ 1.84%, and NA→ 1.79%. In this case, the minimum THD is obtained for NA. The 11th and 13th harmonic are lower during the negative arrangement of hybridization with respect to other abovementioned cases. The maximum delta variation of the RMS ΔV is 36.06 V, which depends on the general voltage reduction noted for the examined case.

In Fig. 20, the transitory of the current of the damper winding is not completed. However, the current values are low. The damper winding losses at no-load conditions are PA→ 84.84 W, J=0→ 82.20 W, and NA→ 79.08 W, while for full load operation are PA→ 150.12 W, J=0→ 150.84 W, and NA→ 151.68 W. Only for this condition the losses are a reverse trend concerning the hybridization arrangement. The maximum force for braking during perturbations is 1576.4 N.

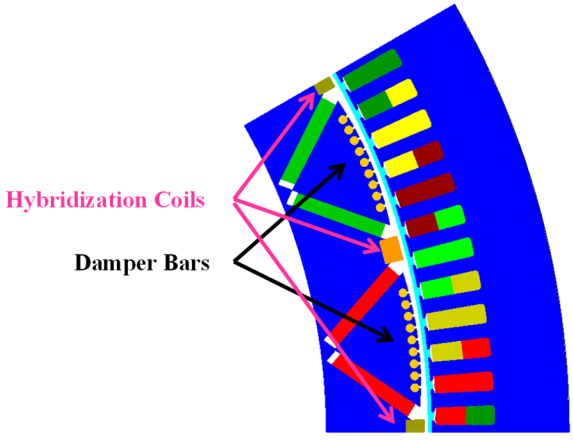

Fig. 18. HPMSG with 9 damper bars with delayed activation of hybridization

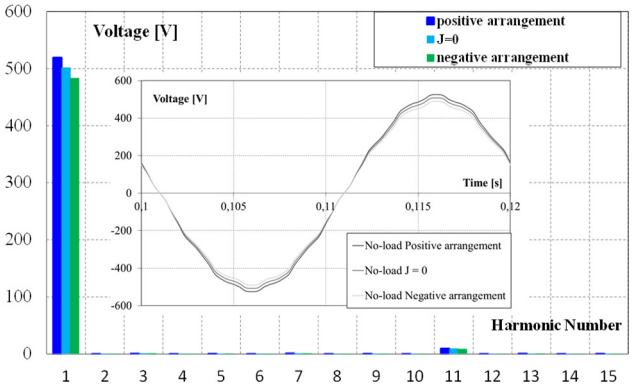

Fig. 19. No-load linked voltage and relative harmonic content for HPMSG with 9 damper bars with delayed activation of hybridization

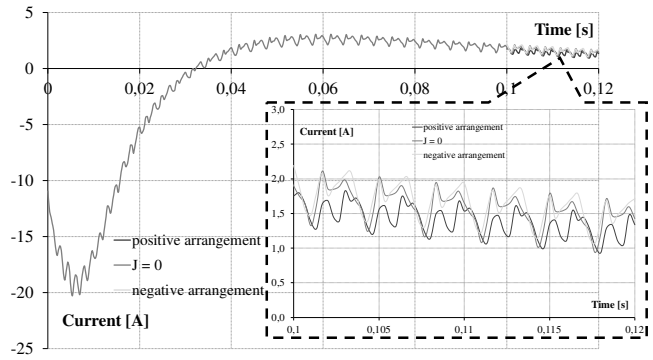

Fig. 20. Total current of the damper cage in the case of 9 damper bars with delayed activation of hybridization

IV. Results Discussion

A comparison of the results was made, taking into account THD, damper cage joule losses, and braking force. The no-load operation has been selected to summarize the results. For THD values (Fig. 21), it is possible to note the lowest value for the case where hybrid coils are used as the damper winding, but thermal issues afflict that configuration, so it cannot be employed. The following good solution is represented by 5 damper bars with delayed activation of hybridization. The THD remains between 1.54÷1.67%, which is a promising result. The next potential solution is represented by 9 damper bars.

For joule losses in the damper windings, the comparison is made in Fig. 22. The very low value is again obtained for the first case, but as mentioned above, that configuration can't be applied. The configuration with a minor number of damper bars has lower damper cage losses. On the other hand, the damper cage losses are very small compared to rated power, about 0.1%.

The produced forces by the damper cage to limit and exhaust the perturbation are compared in Fig. 23. The maximum force is obtained for 5 damper bars design. The second force is recorded d for the system with hybrid and damper windings connected in the same circuit; however, such configuration suffers from high temperature produced by damper cage current during the perturbation.

In the end, the best design for an HPMSG with a damper cage is represented by 5 damper bars. It is important to note that the number of bars can affect the THD values and losses, and a hydroelectric generator always has a damper cage.

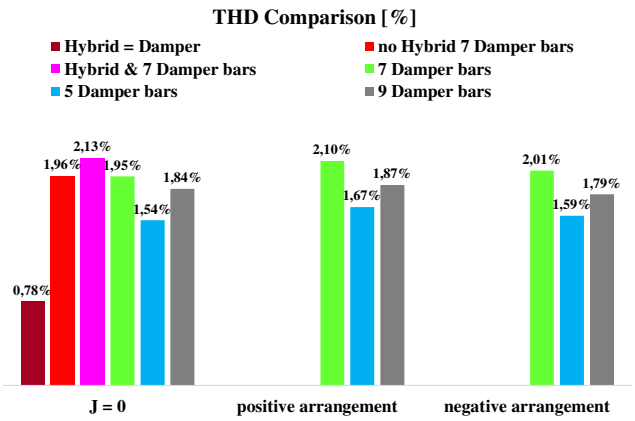

Fig. 21. THD comparison considering hybridization state

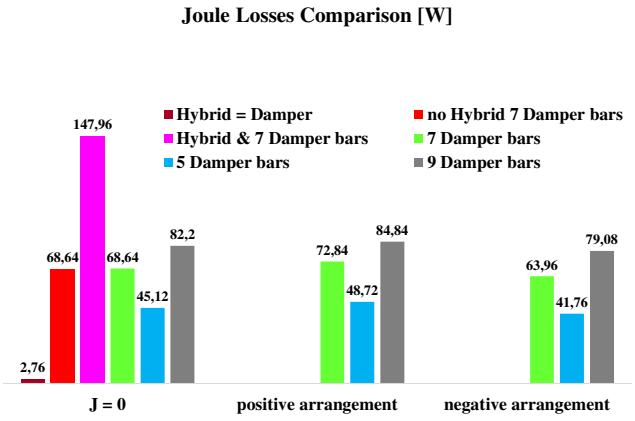

Fig. 22. Comparison of joule losses in the damper windings considering hybridization state

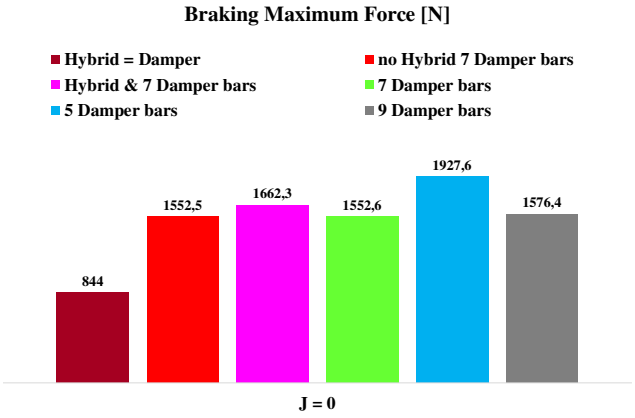

Fig. 23. Comparison of the maximum force for braking during perturbations

V. Conclusions

Different designs of HPMSG with damper cages have been proposed. Several parameters have been investigated to select the appropriate design: harmonic content, THD, damper cage current and losses, and Lorentz force. The configuration with 5 damper bars and delayed activation of hybridization shows the best results. Also, the delta variation of the RMS ΔV is maximum for the selected design. The transitory damper cage current for the promising case does not generate thermal problems. In the end, it is demonstrated that the use of hybridization coils in the generators must consider the damper cage and control strategy.

For future activity, the reduction of the slotting effect through distance variation between the same number of the damper bars or using the magnetic wedge will be investigated. Also, the control strategy will be planned in detail.

ACKNOWLEDGMENT

This study was supported by the National Recovery and Resilience Plan (NRRP), Mission 4 Component 2 Investment 1.3 - Call for Tender No. 341 dated 15.03.2022 of Ministero dell'Università e della Ricerca (MUR); funded by the European Union – NextGenerationEU. Project code PE0000021, Concession Decree no. 1561 of 11.10.2022 adopted by Ministero dell'Università e della Ricerca (MUR), CUP - E13C22001890001 - Project title ``Network 4 Energy Sustainable Transition – NEST". It was also carried out within the Ministerial Decree no. 1062/2021 and received funding from the FSE REACT-EU - PON Ricerca e Innovazione 2014-2020. This manuscript reflects only the authors' views and opinions, neither the European Union nor the European Commission can be considered responsible for them.

REFERENCES

[1] L. Cinti, N. Bianchi, "Hybrid-Excited PM Motor for Electric Vehicle," *Energies* 2021, 14, 916.

[2] K. Kamiev, A. Parviainen, J. Pyrhönen, "Hybrid excitation synchronous generators for small hydropower plants," *IEEE ICEM Conf.*, Lausanne Switzerland, 2016, pp. 2529-2535.

[3] X. Zhao, J. Jiang, S. Niu, Q. Wang, "Slot-PM-Assisted Hybrid Reluctance Generator With Self-Excited DC Source for Stand-Alone Wind Power Generation," *IEEE Trans. on Magn*., vol. 58(2), pp. 1-6, Feb. 2022, Art no. 8700106.

[4] L. Huang, M. Chen, L. Wang, F. Yue, R. Guo, X. Fu, "Analysis of a Hybrid Field-Modulated Linear Generator For Wave Energy Conversion," *IEEE Trans. on App. Supercond*., vol. 28(3), pp. 1-5, April 2018, Art no. 0601205.

[5] L. Ferraris, E. Poskovic, F. Franchini, "Study of the Compositions of Hybrid Magnetic Composite (HMC) Materials for Sensor Applications," *IEEE EPE'18 ECCE Europe Conf.*, Riga, Latvia, 2018, pp. P.1-P.10.

[6] L. Ferraris, F. Franchini, E. Pošković, "Hybrid magnetic composite (HMC) materials for sensor applications," *IEEE SAS Conf*., Catania, Italy, 2016, pp. 1-6.

[7] M. A. Darmani, E. Pošković, F. Franchini, L. Ferraris, A. Cavagnino, C. Gerada, "AFPM Machines Equipped with Multilayer Magnets," *IEEE Trans. on Ener.Conv*., 2024.

[8] F. Graffeo, O. Stiscia, S. Vaschetto, A. Cavagnino, A. Tenconi, "Doubly Excitated Synchronous Machines for Traction Applications," *IEEE ISIE Conf*., Kyoto, Japan, 2021, pp. 1-8.

[9] D. Borkowski, "Small Hydropower Plant as a supplier for the primary energy consumer," *IEEE EPE Conf*., Kouty nad Desnou, Czech Rep., 2015, pp. 148-151.

[10] T. Wegiel, D. Borkowski, "Variable speed small hydropower plant," *IEEE PEDG Conf*., Aalborg, Denmark, 2012, pp. 167-174.

[11] A. Binder, T. Schneider, "Permanent magnet synchronous generators for regenerative energy conversion - a survey," *IEEE EPE ECCE Europe Conf*., Dresden, Germany, 2005, pp. 10 pp.-P.10.

[12] Z. Zhou et al., "Permanent magnet generator control and electrical system configuration for Wave Dragon MW wave energy take-off system," *IEEE ISIE Conf*., Cambridge, UK, 2008, pp. 1580-1585.

[13] E. W. Kimbark, "Damper Windings and Damping," in *Power System Stability, IEEE*, 1995, pp.214-246.

[14] A. M. Knight, H. Karmaker, K. Weeber, "Use of a permeance model to predict force harmonic components and damper winding effects in salient-pole synchronous machines," *IEEE Trans. on Ener. Conv.*, vol. 17(4), pp. 478-484, Dec. 2002.

[15] S. Nuzzo et al., "A Methodology to Remove Stator Skew in Small–Medium Size Synchronous Generators via Innovative Damper Cage Designs," *IEEE Trans. on Ind. Electron*., vol. 66(6), pp. 4296-4307, June 2019.

[16] S. Berhausen, "The influence of the damper cage on the waveforms and subtransient reactances calculated at a two-phase short circuit of a large hydrogenerator," *IEEE WZEE Conf*., Zakopane, Poland, 2019, pp. 1-6.

[17] S. Nuzzo, M. Galea, C. Gerada, D. Gerada, A. Mebarki, N. L. Brown, "Damper cage loss reduction and no-load voltage THD improvements in salient-pole synchronous generators," *IET PEMD Conf*., Glasgow, UK, 2016, pp. 1-7.

[18] Y. Wang, S. Nuzzo, C. Gerada, H. Zhang, W. Zhao, M. Galea, "Integrated Damper Cage for THD Improvements of Variable Speed Salient-Pole Synchronous Generators for the More Electric Aircraft," *IEEE Trans. on Transp. Elect*., vol. 8(3), pp. 3618-3629, Sept. 2022.

[19] S. Nuzzo, M. Degano, M. Galea, C. Gerada, D. Gerada, N. Brown, "Improved Damper Cage Design for Salient-Pole Synchronous Generators," *IEEE Trans. on Ind. Elect*., vol. 64 (3), pp. 1958-1970, March 2017.

[20] A. Hussain, Z. Baig, W.T. Toor, U. Ali, M. Idrees, T.A. Shloul, Y.Y. Ghadi, H.K Alkahtani, "Wound Rotor Synchronous Motor as Promising Solution for Traction Applications", *Electronics*, 2022, 11, 4116.

[21] Chunting Mi, M. Filippa, J. Shen, N. Natarajan, "Modeling and control of a variable-speed constant-frequency synchronous generator with brushless exciter," *IEEE Trans. on Ind.App*., vol. 40 (2), pp. 565-573, March-April 2004.

[22] E. Illiano, "A separately excited synchronous motor as high efficient drive in Electric Vehicles", *ATZ Elektron Worldw* 8, 2013, pp. 44-49.

[23] J. K. Nøland, F. Evestedt, J. J. Pérez-Loya, J. Abrahamsson, U. Lundin, "Testing of Active Rectification Topologies on a Six-Phase Rotating Brushless Outer Pole PM Exciter," *IEEE Trans. on Ener. Conv*., vol. 33(1), pp. 59-67, March 2018.

[24] H. M. Woo, D. -H. Lee, "Starting and Dynamic Performance of A Parallel Field Rotor Type Hybrid Generator with PM Exciter," *IEEE ICIT Conf.*, Melbourne, Australia, 2019, pp. 317-322.

[25] S. Nuzzo, P. Bolognesi, C. Gerada, M. Galea, "Simplified Damper Cage Circuital Model and Fast Analytical–Numerical Approach for the Analysis of Synchronous Generators," *IEEE Transs on Ind. Electron*., vol. 66(11), pp. 8361-8371, Nov. 2019.

[26] A. Darabi, C. Tindall, "Damper cages in genset alternators: FE simulation and measurement," *IEEE Trans. on Ener. Conv*., vol. 19(1), pp. 73-80, March 2004.

[27] H. Castro-Coronado, J. Antonino-Daviu, A. Quijano-López, V. Fuster-Roig, P. Llovera-Segovia, "Evaluation of the Detectability of Damper Cage Damages in Synchronous Motors through the Advanced Analysis of the Stray Flux," *IEEE ECCE Conf*., Detroit, USA, 2020, pp. 2058-2063.